Membrane Water Treatment, *Vol. 7, No. 2 (2016) 155-173*
DOI: http://dx.doi.org/10.12989/mwt.2016.7.2.155

Development of blend membrane by sulfonated polyethersulfone for whey ultrafiltration

Fatemeh Esfandian [1], Majid Peyravi [*1],
Ali Asqar Qoreyshi [1] and Mohsen Jahanshahi [1]

Membrane Research Group, Nanobiotechnology Institute, Babol University of Technology, Babol, Iran

(*Received September 27, 2015, Revised December 16, 2015, Accepted December 28, 2015*)

Abstract. The present work has been focused on the development of polysulfone (PSf) ultrafiltration membrane via blending by sulfonated polyethersulfone (SPES) in order to permeability enhancement for ultrafiltration of cheese whey. In this regards, sulfonation of polyethersulfone was carried out and the degree of sulfonation was estimated. The effect of blend ratio on morphology, porosity, permeation and fouling of PSf / SPES membranes was investigated. Filtration experiments of whey were conducted for separation of macromolecules and proteins from the lactose enrichment phase. The morphology and performance of membranes were evaluated using different techniques such SEM, AFM, and contact angle measurements. The contact angle measurement showed that the hydrophilicity of membrane was increased by adding SPES. According to AFM images, PSf / SPES membranes exhibited lower roughness compared to neat PSf membrane. The water and whey flux of these membranes were higher than neat membrane. However, flux was decreased when the PSf / SPES blend ratio was 0/100. It can be attributed to pore size and morphology changes. Further, fouling parameters of PSf membrane were improved after blending. The blend membranes show a great potential to be used practically in proteins separation from cheese whey.

Keywords: sulfonation; PSf / SPES membranes; blending; proteins separation; cheese whey

1. Introduction

Whey is the main by-product of the dairy industry which is obtained during cheese production by coagulating and separating casein and proteins from milk (Pan *et al*. 2011). Whey contains a high content of valuable components with total solids of about 6%. The solids are basically consisted by 80% lactose and 10-12% proteins (Suárez *et al*. 2006, Yorgun *et al*. 2008, De Souza *et al*. 2010, Hinkova *et al*. 2012). The presence of high amount of lactose at whey is introduced it as a rich source of lactose. With recovery of lactose from whey, lactose can be used in the food, dairy and drug industries and can be either directly fermented or hydrolyzed to produce glucose and galactose (Das *et al*, 2015). Furthermore, this strategy can achieve an adequate removal of BOD and COD from cheese whey to close standard permit for a wastewater discharge and dissolves wastewater treatment problem (Yang and Silva 1995, Rice *et al*. 2009). In order to recovery of lactose, it is initially necessary to remove the proteins of whey to improve the purity of lactose stream. Ultrafiltration (UF) process is one of the efficient ways that have been used for

*Corresponding author, Professor, E-mail: majid.peyravi@nit.ac.ir

 ISSN: 2005-8624 (Print), 2092-7037 (Online)

separation of whey proteins and purification of lactose (Rahimpour *et al*. 2009b). The wide spread use of ultrafiltration has opened up new markets for whey products. The protein stream can be condensed and dried by the same equipment used to process raw whey. Edible protein has found a good market as a food additive or protein supplement (Baldasso *et al*. 2011). This work is focused on the ultrafiltration membranes to separate the protein molecule from the lactose sugar and other molecules in the whey. Because of the importance of permeate flux and fouling limitations on the membrane surface, making membrane with appropriate surface chemistry, roughness, average pore size and porosity is key step in UF process.

The morphology and structural properties (porosity and mean pore size) of membrane will be affected by adding inorganic salts in the casting solution. Lithium chloride (LiCl) has been considered as a good candidate of inorganic salts to improve the surface quality for membrane preparation. Because the organic salts strongly interact with carbonyl groups in polar solvents such as dimethylformamide and the formed complexes would increase the viscosity of casting solution (Bottino *et al*. 1988, Shibata *et al*. 2000, Wang *et al*. 2000, Lee *et al*. 2002).

It is worthy of notice that one of the major problems associated with UF processes applied in dairy industry is membrane fouling. Proteins are the main foulants responsible for membrane fouling among the different substances in whey. Membrane fouling will remarkably deteriorate membrane performance and consequently result in a gradual flux decline with time during filtration and high energy consumption (Faibish and Cohen 2001, Argüello *et al*. 2003, James *et al*. 2003, Mohammadi *et al*. 2003, Corbatón-Báguena *et al*. 2015). Particle size distribution is a key factor controlling the mechanism of membrane fouling (Costa *et al*. 2006). Particles smaller than the membrane pore size penetrate inside membrane pores and may adsorb into the pore, reducing the effective size of pores or completely blocking the pores. While other molecules which are deposited on the membrane surface form a cake layer. Therefore, two essential mechanisms can be considered for membrane fouling (pore blockage and cake filtration) (Ma *et al*. 2000, Indok Nurul Hasyimah *et al*. 2011, Corbatón-Báguena *et al*. 2015). One effective way to enhance membrane performance and decrease membrane fouling is increment of the membrane surface hydrophilicity (Pieracci *et al*. 1999, Alpatova *et al*. 2013). Many attempts had been done in order to reduce the hydrophobicity of membrane and minimize the membrane fouling. In order to increase membrane hydrophilicity, different strategies can be used such as plasma treatment, UV induced graft polymerization and blending of hydrophilic additives in a membrane casting solution (Rahimpour *et al*. 2009a, Rahimpour *et al*. 2010b, Alpatova *et al*. 2013, Zhao *et al*. 2013, Sinha and Purkait 2015).

The modification of PSf through blending hydrophilic agent may effectively improve the structural properties and fouling of PSf membrane to increase the flux of membrane. Sulfonated polymers were considered to be much more resistant to the fouling due to the formation hydrophilic groups of SO_3H along the polymer backbone by which the hydrophilicity of sulfonated polymer increased. Sulfonated PES (SPES) can be blended to PSf in the casting solution as a hydrophilic modifier in order to enhanced hydrophilicity of membrane and prevent proteins from binding to the membrane surface and pores (Blanco *et al*. 2001, Xing *et al*. 2004). A novel hydrophilic poly (vinylidene fluoride)/poly (p-phenylene terephthalamide) (PVDF/PPTA) blend membrane was prepared via in situ polycondensation of p-phenylene diamine (PPD) and terephthaloyl chloride (TPC) in PVDF solution by Li *et al*. (2015). Hydrophilicity and antifouling properties of the in situ blend membranes were greatly improved than pure PVDF membrane.

Considering the membrane upgrading with antifouling properties, the objectives of this research fall into three basic issues: (i) developing structural surface parameters of PSf membrane

through adding LiCl in order to reduce the negative impact of non-uniform pore size in terms of pores blocking mechanism. (ii) Improving membrane surface chemistry through blending with sulfonated PES relying on hydrophilicity to decline the cake layer thickness. (iii) Assessment of the feasibility of the modified membranes for whey Ultrafiltration. In this regards, PES was sulfonated with sulfuric acid and then different concentrations of SPES were blended directly with PSf to improve the hydrophilicity of the membrane. The performance of the developed membranes containing LiCl and SPES was investigated by measuring the permeability of pure water and whey. In addition, fouling phenomenon was analyzed by varying the surface properties of membrane in terms of both pore blockage and cake filtration mechanisms.

2. Experimental

2.1 Material

Polysulfone (PSF, *Mw* = 35,000 g/mol, Density = 1.24 g/mL at 25℃, Solvay polymers) and Polyethersulfone (PES) (Ultrason E 6020 P, *Mw* = 58,000 g/mol) were used as polymer for the preparation of the ultrafiltration membrane. Sulfuric acid was used as solvent and reactant from Merck. Polyvinylpyrrolidone (PVP, with *Mw* = 25,000 g/mol, Density = 1.2 g/mL at 20℃), LiCl and N, N dimethylformamide (DMF) as solvent were supplied from Merck. Whey was supplied from kalleh factory dairy products (Amol-Iran).

2.2 Sulfonation method of PES

Sulfonation of PES by sulforic acid (98%) as sulfonating agent and solvent was performed. A 100 ml glass reactor, equipped with a magnetic stirrer and a nitrogen inlet/outlet was charged with PES pellet, and sulfuric acid (98%). The temperature for polymer dissolution was 25℃. The reaction was allowed to proceed for 3 h and then SPES was gradually precipitated into ice-cold de-ionized water under stirring. The resulting precipitate was recovered by filtration and washed multiple times with de-ionized water until pH became approximately 5-6. In this study, the sulfonated PES was insoluble in water and was totally recovered via precipitation separation by filtration. Finally, the SPES was dried under vacuum at 40℃ overnight (Xing *et al*. 2004, Rahimpour *et al*. 2010b).

2.3 Characterization of SPES

The degree of sulfonation (DS) was calculated from the ion exchange capacity (IEC) of the prepared SPES. IEC capacities were measured using a titration method. For this purpose, 0.3 g of SPES was suspended in 30 ml of 2 M NaCl solution for 24 h to liberate the H^+ ions and then titration was done with standardized 0.1 M NaOH solution using phenolphthalein as an indicator. The IEC indicates the ratio of exchanged H^+ to the weight of the dried polymer. The IEC was calculated according to this equation

$$IEC(mequiv./g) = \frac{a \times b}{W_{dry}} \quad (1)$$

Where a is the normality of NaOH solution used (mequiv.ml^{-1}), b is the volume of NaOH

solution used (ml) and w_{dry} is the dry weight of the polymer (Klaysom *et al*. 2011). DS is the fraction of monomer unit of PES which is sulfonated (ion exchangeable) after reaction. The average sulfonation degree (DS) can be measured from the IEC, if we assume that all the sulfonic groups in the film are available (i.e., ion exchangeable). So that, the average number of DS is equal to the ratio of DS to IEC as follow

$$DS = \frac{M_0 \times IEC}{1000 - 103 \times IEC} \tag{2}$$

Where M_0 232 g/mol is the mass unit of the polymer and 103 is the molar mass of the SO_3Na group (Rahimpour *et al*. 2010b).

2.4 Preparation of ultrafiltration membranes

The flat sheet membranes were prepared by phase inversion via immersion precipitation technique. At the first step, the polymeric solution was prepared by dissolving certain amounts of sulfone polymers and 1wt.% of PVP in DMF. In parallel, 0.5 wt.% LiCl was dissolved at DMF separately by magnetic stirrer for 1 h. Then, the mixture of LiCl and DMF were mixed with polymeric solution at the temperature of 60℃ for 12 h with a magnetic stirring to attain homogenous casting solution. The solution was sprinkled and cast on the polyester non-woven fabric using a homemade casting knife with 70 μm thickness. The cast film was immediately immersed in the precipitation (coagulation) bath including deionized water to initiate the phase inversion. The prepared membranes were washed and stored at 25℃ distilled water for 1 day to completely leach out the residual solvents and additives. As the final stage, the membranes were dried by placing between two sheets of filter paper for 24 h at room temperature. The compositions of the casting solution were given at Table 1.

2.5 Characterization of membranes

The morphological studies were accomplished by atomic force microscopy (AFM) and scanning electron microscopes (SEM). AFM device was a Nanosurf scanning probe optical microscope (EasyScan II, Swiss). The surface roughness parameters of the composite membranes which are expressed in terms of the mean roughness (*Sa*), the root mean square of the Z data (*Sq*) and the mean difference between the five highest peaks and lowest valleys (*Sz*) were calculated from AFM images using tapping mode method via Nanosurf EasyScan software at a scan area of 5 μm × 5 μm. Scanning electron microscopes (SEM) were used to inspect the cross-section and surface of membranes. The model of SEM apparatus was Vega; (ii) Tescan. The membranes were

Table 1 Composition of casting solution

Membrane	PSf/SPES composition (w/w)	PSf (wt.%)	SPES (wt.%)	LiCl (wt.%)	PVP (wt.%)	DMF (wt.%)
M_0	100/0	16	0	0.5	1	82.5
M_{50}	50/50	8	8	0.5	1	82.5
M_{75}	25/75	3.2	12.8	0.5	1	82.5
M_{100}	0/100	0	16	0.5	1	82.5

cut into pieces of small sizes and cleaned with filter paper. These pieces were immersed in liquid nitrogen for 10-15 s and were frozen. Frozen bits of the membranes were broken and kept in air for drying. These dry samples were gold sputtered for producing electric conductivity, and photomicrographs were taken in very high vacuum conditions at 10 and 25 kV.

To study the wetting property of the membrane surface as a function of SPES concentration in the casting solution, water contact angle was measured for evaluation of the membrane hydrophilicity using a contact angle measuring instrument [G10, KRUSS, and Germany]. De-ionized water was used as the probe liquid in all measurements. To minimize the experimental error, the contact angle was measured at five random locations for each sample and the average value was reported.

Equilibrium water content (EWC) is considered to be a main characterization parameter that indicates the degree of hydrophilicity and hydrophobicity of a membrane (Arthanareeswaran *et al*. 2006). Also it is relative to the porosity of a membrane. EWC was determined after soaking of membranes in the water for 24 h. Membranes were weighed in an electronic balance under wet status after mopping the surface water with blotting paper. The wet membranes were dried by placing in a vacuum oven for 24 h at a temperature of 50-60℃ and for another time they were weighed in dry state. Then EWC was calculated as follow

$$\mathrm{EWC}(\%)=\frac{W_w - W_d}{W_w}\times 100 \tag{3}$$

Where *Ww* is wet membranes weight (g) and W_d is dry membranes weight (g).

The membrane porosity ε is the ratio of the volume of pores to the total volume of the porous membrane and is obtained by Eq. (4) (Chakrabarty *et al*. 2008)

$$\varepsilon=\frac{W_w - W_d}{\rho_w \times AL} \tag{4}$$

Where, ρ_w is pure water density (kg/m^3) at room temperature. *A* and *L* are membrane area and membrane thickness, respectively.

The membrane mean pore radius (r_m) was measured by the pure water flux and porosity data. r_m was calculated by the following formula (Wu *et al*. 2008).

$$r_m=\sqrt{\frac{(2.9-1.75\epsilon)\times P(8\eta lQ)}{\epsilon\times A\times \Delta P}} \tag{5}$$

Where η is the water viscosity (8.9×10^{-4} Pa·s), Q is water flux (m^3/s), ΔP is the operation pressure (3×10^5 Pa) and l is the membrane thickness

2.6. Filtration performance and fouling analysis

The filtration experiments were conducted using a laboratory-scale dead-end system at temperature of 25℃ and pressure of 3 bar. The dead-end system is depicted in Fig. 1. The feed flow was passed through the membrane by pressure driving force which was provided by compressed nitrogen gas cylinder. Membrane with radius of 5 cm was fixed between two steel parts and also was sealed with an O-ring. A magnetic stirrer was also located under the membrane

cell to stir feed in order to prevention of the concentration polarization. After the membrane was fixed, the stirred cell and the solution reservoir were filled with deionized water to measure the pure water flux (J_{w0}). After 15 min filtration, the feed solution containing whey from kalleh was switched, and the flux (J_p) was evaluated. Finally, the cell and the solution reservoir were fully emptied and refilled with deionized water. The membrane was washed with deionized water for 10 min and the water flux (J_{w1}) was measured again. Fluxes of different membranes were calculated as follow

$$J = \frac{m}{A.\Delta t} \tag{6}$$

Where, m is the mass of permeate, A is the membrane area and Δt is the permeation time. The protein rejection ratio was calculated following the equation below

$$R(\%) = \left(1 - \frac{C_p}{C_f}\right) \times 100 \tag{7}$$

Where C_p and C_f represented the proteins concentrations in permeate and feed solutions, respectively. The following method was used for determining the proteins content in permeate and feed.

Among the proteins in whey (beta-lactoglobulin, alpha-lactalbumin, bovine serum albumin and immunoglobulins), beta-lactoglobulin contains 65% of total proteins. Regarding to the high concentration of beta-lactoglobulin in whey, this protein is chosen as a characteristic protein in our experiment and the protein concentration was measured by UV–vis spectrometer at wavelength of 287 nm.

Fouling can be quantified by the resistance appearing during the filtration and cleaning can be specified by the removal of this resistance. The resistance is due to the formation of a cake or gel layer on the membrane surface. In order to evaluate the fouling-resistant capability of the membrane, the flux recovery ratio (FRR) was calculated using the following expression

$$FRR(\%) = \frac{J_{w1}}{J_{w0}} \times 100 \tag{8}$$

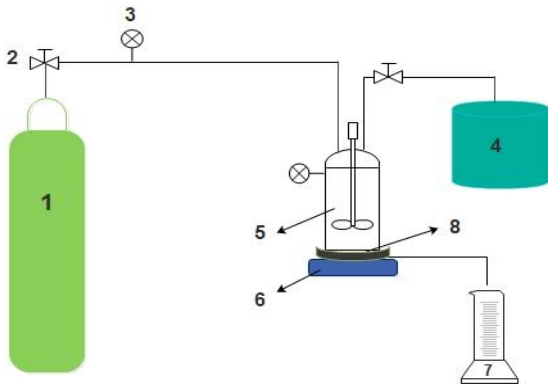

Fig. 1 Exhibition of dead-end filtration system: 1-cylinder with compressed nitrogen; 2-pressure safety valve; 3-pressure gauge; 4-feed tank; 5-membrane cell; 6-magnetic stirrer; 7-permeate collector; 8-the collection where the membrane placed

The fouling-resistant capability of the membrane was described by

$$R_t = \frac{J_{w0} - J_p}{J_{w0}} \tag{9}$$

Where R_t is the degree of total flux loss caused by total fouling. Reversible fouling ratio (R_r) and irreversible fouling ratio (R_{ir}) were also defined and calculated by following equations, respectively.

$$R_t = \frac{J_{w1} - J_p}{J_{w0}} \tag{10}$$

$$R_{ir} = \frac{J_{w0} - J_{w1}}{J_{w0}} \tag{11}$$

Obviously, R_t was the sum of R_r and R_{ir}.

3. Results and discussion

3.1 Effect of LiCl additive

Relying on upgrading the structural surface properties of the PSf membrane, different concentration of LiCl (0, 0.1, 0.5 and 1 wt.%) were utilized to determine the optimal concentration of LiCl. For this reason, the porosity and mean pore size of these membranes were estimated and shown in Fig. 2. It was observed that, the porosity of membranes with LiCl was improved after addition of LiCl in the casting solution. . In contrast, a decrement in the mean pore size of membranes was indicated by increasing LiCl to 1 wt.%.

This trend is associated with the thermodynamic and kinetic effects of the PSf dope system before and after LiCl addition. It can be visually seen that the viscosity of dope solution increases when the concentration of LiCl increases from 0.1 to 1 wt.%. It may be correlated to the interaction between ions of LiCl and DMF that formed complexes (Kesting 1965, Wang *et al*. 2015). In fact, increasing LiCl concentration increased the thermodynamic instability of the dope

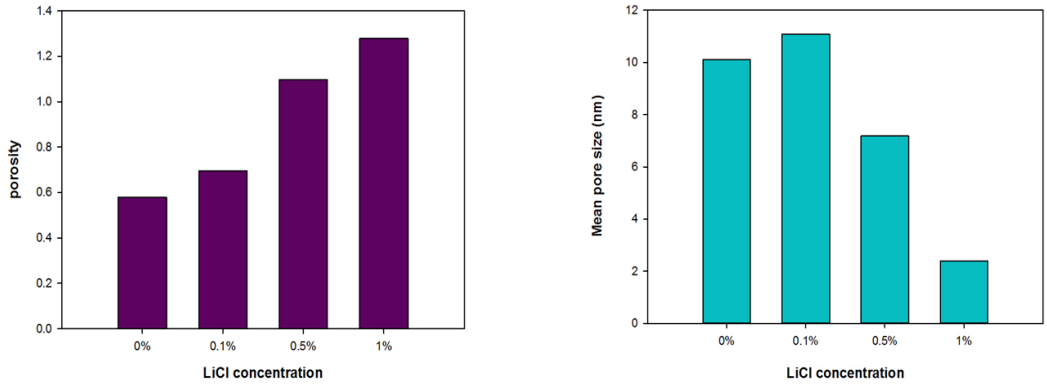

(a) (b)

Fig. 2 Porosity (a) and mean pore size (b) of prepared membranes with different concentration of LiCl

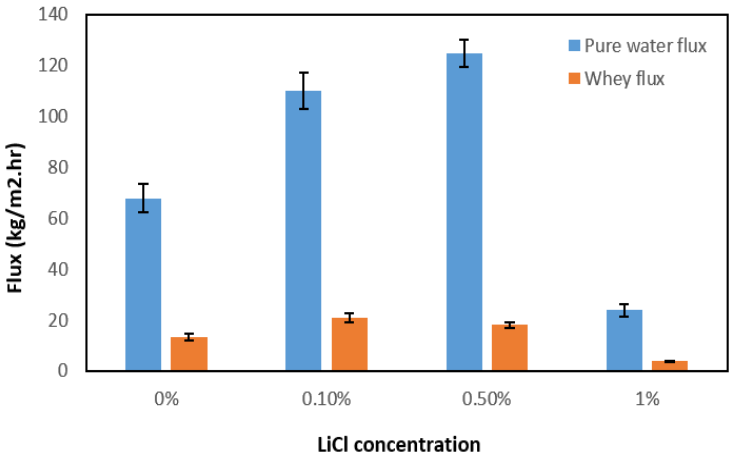

Fig. 3 Effect of LiCl concentration on pure water and whey flux

solution which can facilitate a rapid phase demixing by the formed complexes. On the other hand, the complex formed as the strong interactions between inorganic salt and solvent of the casting solution tended to delay the dope precipitation as a kinetic effect, which partially offset the thermodynamic impact of LiCl addition. As a result, the size of the surface pores in the fabricated membranes is reduced at high LiCl dosage in the casting solution (Lalia *et al*. 2013).

The pure water and whey flux of membranes with different concentration of LiCl by using dead- end system were also measured and shown in Fig. 3. Both the flux of pure water and whey for modified membranes were higher than a membrane without LiCl except for membrane including 1 wt.% LiCl. Among the membranes, a maximum value of pure water flux was observed for the membrane with 0.5 wt.% LiCl. This may be due to higher porosity after modification of membrane by addition of LiCl. The authors believe that severe flux decline of membrane including 1 wt.% LiCl is attributed to the dominant effect of pore size decline than the porosity enhancement. However, the whey flux for modified membrane was decreased with increase in LiCl concentration. This may be interpreted with the protein fouling of whey filtration. Indeed, membranes with smaller pore size are more preferable for pore blocking during whey filtration. It can be concluded that the 0.5 wt.% LiCl is optimum concentration of additive because of appropriate porosity and pore size and higher value of pure water flux.

3.2 Mechanism of PES sulfonation

Sulfonated PES was synthesized to modify the properties of PSf membrane. In our work, concentrated sulfuric acid (98%) was used to introduce the negatively charged sulfonate group (SO_3H) onto the benzene ring of PES. Fig. 4 represented the synthesize steps of the sulfonated PES. The sulfonated process for PES is based on the electrophilic substitution reaction. According to PES structure, the O = S = O group linked to benzene ring is electrophilic. Moreover, as for the effect of metha position, the substitution reaction only occurred in the metha position of joint of the benzene ring and O = S = O group. The reaction time and the ratio of sulfonating agent and polymer value influenced on degree of sulfonation. The degree of sulfonation (DS) was determined by titration process. The value of DS = 0.467 was calculated using Eq. (2).

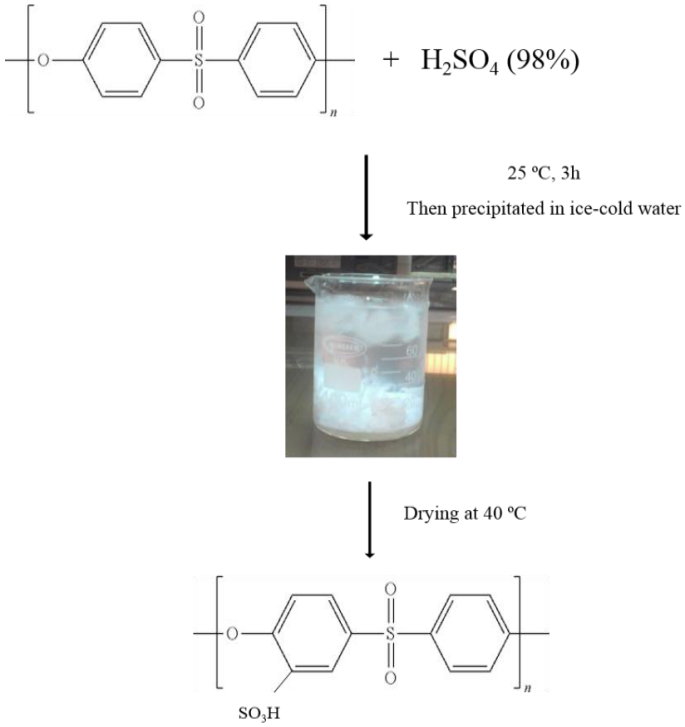

Fig. 4 Synthesize mechanism of sulfonated PES

Fourier transform infrared spectra confirmed the presence of sulfonic acid groups on the blend PSf/SPES (0/100) membrane. As shown in Fig. 5, the peak at 1011 cm^{-1} is attributed to sulfonic acid group (-SO_3H) and indicated the effective presence of SPES in the membrane structure. Furthermore, it is clearly seen that the polar hydroxyl groups (OH) are formed onto the fully SPES membrane which can be confirmed by the adsorption band at 3400 cm^{-1}.

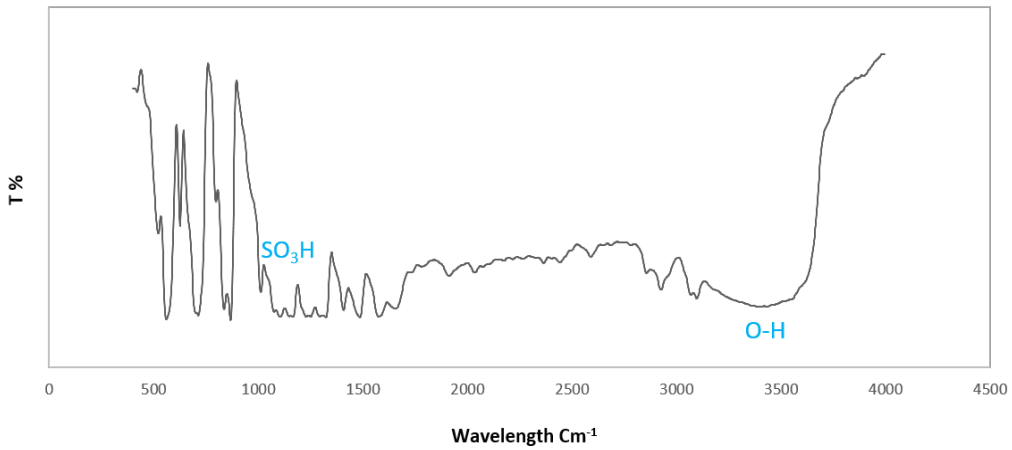

Fig. 5 FTIR spectra of membrane with the ratio of PSf to SPES (0/100)

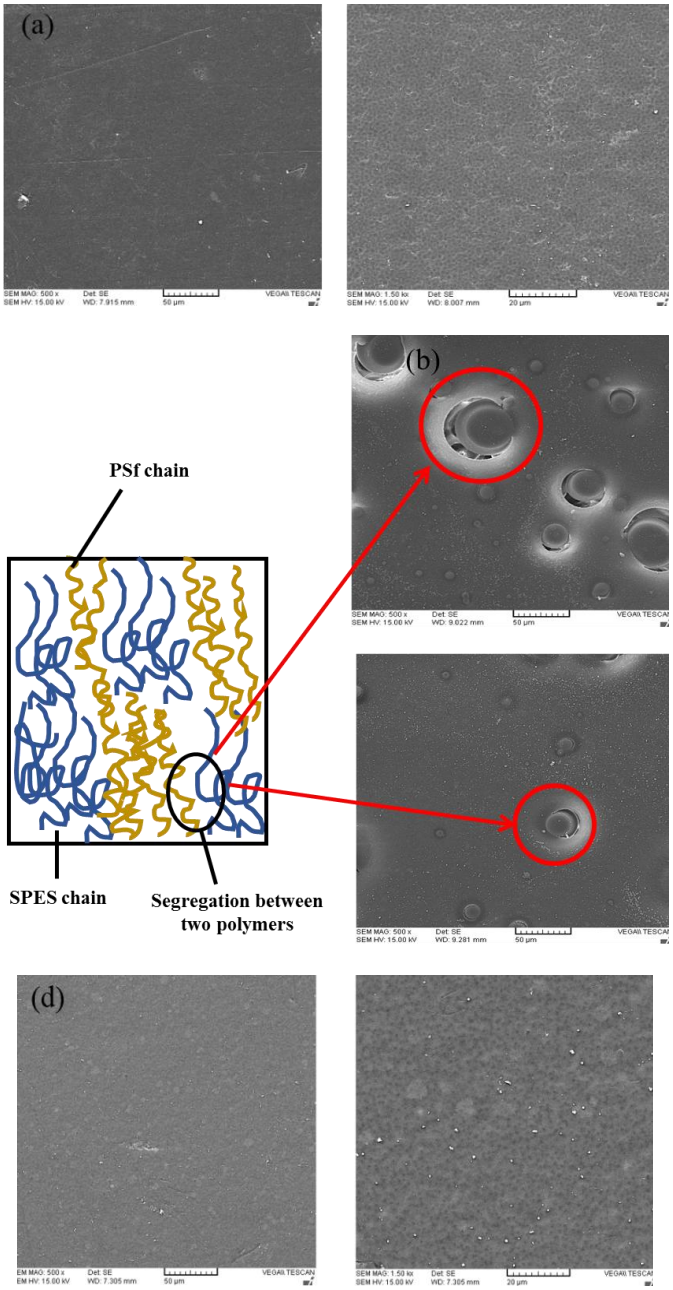

Fig. 6 Surface SEM images of PSf/SPES blend membrane: (a) 100/0; (b) 50/50; (c) 25/75; (d) 0/100

3.3 Morphological study of membranes

The morphologies of the neat and blend ultrafiltration membranes were observed by SEM and the obtained results were shown in Fig. 6 at two magnifications. As shown in Figs. 6(a) and 6(d), the surface of neat PSf and SPES membranes were quite uniform without any defects and the pores

distributed uniformly through the surface. But in the membranes prepared by blending of two polymers (PSf and SPES), this uniformity is not obviously on the membrane surface. The segregation domains can be observed on the surface of blended membrane. It can be ascribed to poor adhesion properties and absence of coordination between PSf and SPES chains, and this poor adhesion increased the immiscible nature of this two polymers (Jacob *et al*. 2014). Moreover, it can be visually seen that the dope solution tended to form two liquid separate phases. The authors believe that it may be due to the difference in solubility of the polymers with solvent. Therefore, the sites where two polymers contact each other resulted in the phase segregation of two different polymers on the surface of M_{50}, and M_{75}. The uniform sites observed on the M_{50}, and M_{75} surfaces can be attributed to the each domain of PSf and SPES. For M_{25}, this was intensified when the ratio of PSf/SPES was 75/25 called as M_{25}. In case of M_{25}, two immiscible liquid phases was formed in the dope solution and casting wasn't performed. The interaction between two different polymers may cause the formation of large pores in the membrane structure. Considering the surface SEM images of all membranes, the white spots were seen on the surface. It may be related to LiCl or PVP particles moved to the membrane surface during phase inversion process.

Cross-sectional SEM images of neat and blend membranes prepared were shown in Fig. 7. It is easy to recognize an asymmetric structure, which is consist of thin and dense skin layer and a

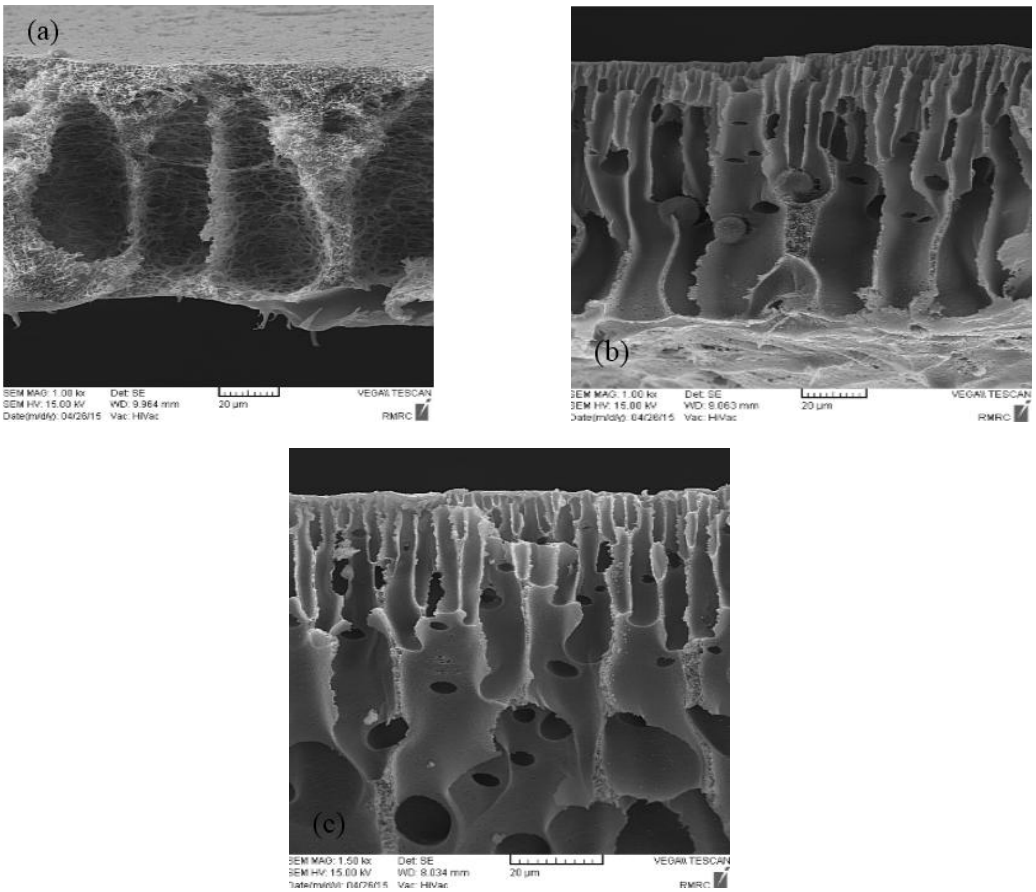

Fig. 7 Cross sectional SEM images of PSf/SPES blend membrane: (a) 100/0; (b) 25/75; (c) 0/100

porous bulk with finger-like and macroviod structure at the bottom. A comparison of SEM images reveals that M_0 has sponge structure with low number of finger-like pores. Whereas, the addition of SPES in the casting solution changes the morphology of membrane and leads to more porous structure with smaller finger-like pores. Moreover, the thickness of dense skin layer significantly increased with increasing the PSf/SPES ratio from 25/75 to 0/100. This alteration in membrane morphology can be explained with the phase inversion mechanism during membrane preparation. There is SO_3H functional group in SPES polymer chains that is strongly hydrophilic (Patri *et al*. 2004). The authors think that at the presence of SPES in the dope solution, the affinity between non-solvent (water) and polymer rich phase increases. As a result, high affinity among two phase is disposed to give instantaneous demixing and this results in membrane with finger-like structure in the sublayer (Qin *et al*. 2013).

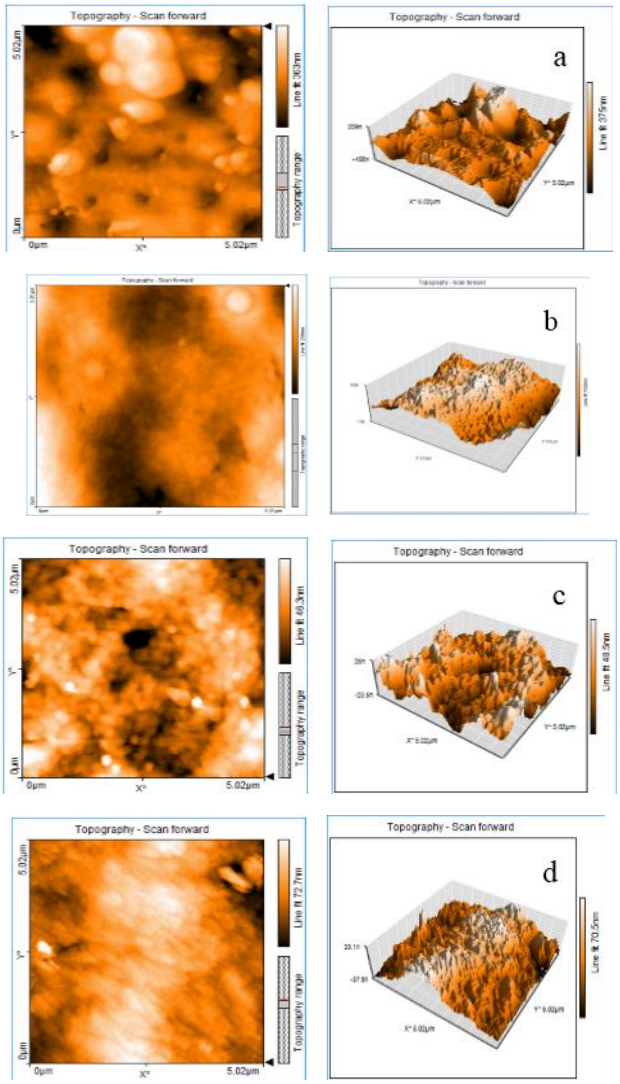

Fig. 8 Two and three-dimensional surface AFM images of PSf/SPES blend membrane: (a) 100/0 M_0; (b) 50/50 M_{50}; (C) 25/75 M_3; (d) 0/100 M_4

Table 2 Porosity and mean pore size of the prepared membranes

Membrane	Porosity	Mean pore size (nm)
M_0	0.4063	5.9
M_{50}	0.7387	7.7
M_{75}	0.9437	4.3
M_{100}	0.8592	4.5

In the present study, the atomic force microscopy (AFM) measurements were used to investigate the surface roughness of the prepared membranes. Fig. 8 indicated the two and three-dimensional AFM images of M_0, M_{50}, M_{75}, and M_{100} surface at a scan size of 5 μm × 5 μm. In these images, the brightest area illustrates the highest point of the membrane surface and the dark regions demonstrate the valleys or membrane pores. The porous structure with segregated domains was observed for membranes.

3.4 Study the surface properties of membranes

In whey protein separation, various macromolecules with various chemical and physical properties exist in the cheese whey, which increase the chance of membrane fouling as soon as whey contacts with membrane even before filtration is started. It is important to know the effect of structural surface parameters such as porosity, membrane pores, hydrophilicity and surface roughness on the whey filtration performance. The porosity and mean pore size information of the prepared membranes are given in Table 2. It can be seen that the porosity of membranes containing SPES were higher than a membrane just including PSf. It seems that the enhancement of thermodynamic instability in the gelation media effects on both driving forces and the relative diffusion rate of the solvent and non-solvent (Qiu *et al*. 2009, Majeed *et al*. 2012). In fact, it may be influence on the rate of solvent outflow and the non-solvent (water) inflow and led to form the membrane with higher porosity at high loading of SPES. It is anticipate that the surface mean pore size of M_{75} is lower than the other membranes due to the higher porosity. Indeed, there is a clear proportionality between pore radius and surface porosity. At the defined area of membrane surface, by reduction of the pore size, the number of pores is increased and this results in a higher porosity (Peyravi *et al*. 2015). However, this trend was not observed for M_{50}. The size of membrane pores depend on the predominant polymer and blended polymer in the casting solution. For M_{50} membrane, due to the same contribution of both polymers (main polymer and blended polymer) in the casting solution, the maximum segregation between two polymers was obtained and this membrane has the largest pore size.

The surface roughness parameters of the membranes that are demonstrated in terms of the mean roughness (S_a), the root mean square of the Z data (S_q) and the mean difference between the highest peaks and lowest valleys (S_z) were calculated and presented in Table 3. The roughness of membrane declined with an increase of SPES in the casting solution. The results indicated that membranes with SPES have smoother surface than a membrane just containing PSf, but a comparison of M_{75} and M_{100} shows that the roughness of M_{100} is higher than M_{75}. As a general low, the variation of pore size is likely affected on the surface roughness. The increase in pore size of membrane caused an increase in membrane roughness (Kiadehi *et al*. 2015). Among these four membranes, M_0 due to larger mean pore size has rougher surface than other membranes.

Table 3 Effect of SPES on roughness and hydrophilicity of membranes

Membrane	Roughness			Contact angle (°)
	S_a (nm)	S_q (nm)	S_z (nm)	
M_0	48.3	65.6	455.6	90
M_{50}	8	9.42	78.2	60
M_{75}	8.1	10	84.2	73.6
M_{100}	11.9	14.3	96	73.2

The contact angles of M_0, M_{50}, M_{75} and M_{100} membranes that specify the membrane surface hydrophilicity were presented in Table 3. It can be seen that the M_{50}, M_{75} and M_{100} membranes have lower contact angle compared to the M_0. The contact angles of M_{50}, M_{75} and M_{100} indicate that these membranes have more hydrophilic surfaces. It is expected that the contact angle of M_{100} must be lower than M_{75} due to the presence of more SO_3H group while this trend was not obtained.

It should be noted that two parameters influenced on the contact angle are hydrophilicity and surface roughness. The surface with more hydrophilicity decrease the contact angle whereas the higher roughness increase it (Jung and Bhushan 2006, Rahimpour *et al*. 2010a). According to Table 3, the surface roughness of M_{100} was higher than M_{75}. It seems that the effect of higher roughness can be dominated to higher hydrophilicity on the contact angle value.

3.5 Effect of SPES on membrane separation properties

Fig. 9 shows the pure water and whey permeation through different fabricated membranes. Comparison the pure water flux of single polymer membranes (M_0, M_{100}) indicated that M_0 have higher pure water flux than M_{100}. This related to the smaller pore size of M_{100} than M_0. But the comparison of whey flux of M_0 and M_{100} showed that flux of M_{100} was slightly higher than M_0. This increase in whey flux was because of improvement surface hydrophilicity of M_{100} by adding SO_3H groups on the membrane surface. By comparing the flux of blended membranes (M_{50}, M_{75}), it was observed high pure water and whey flux for this two membranes. The authors believe that it was because of the segregation between chains of two different polymers according to the surface SEM image that caused to form larger pore size than M_0 and M_{100}.

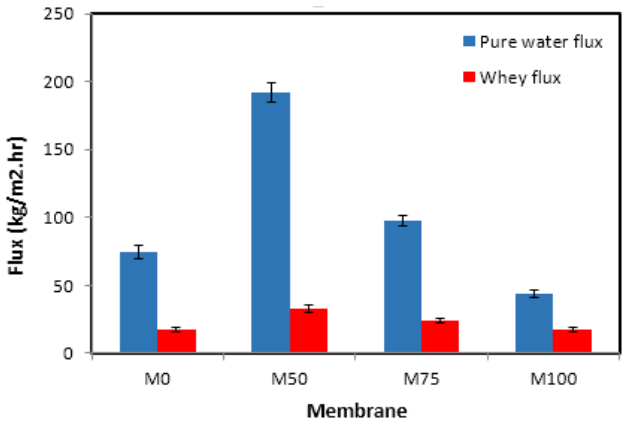

Fig. 9 Pure water and whey flux of prepared membranes

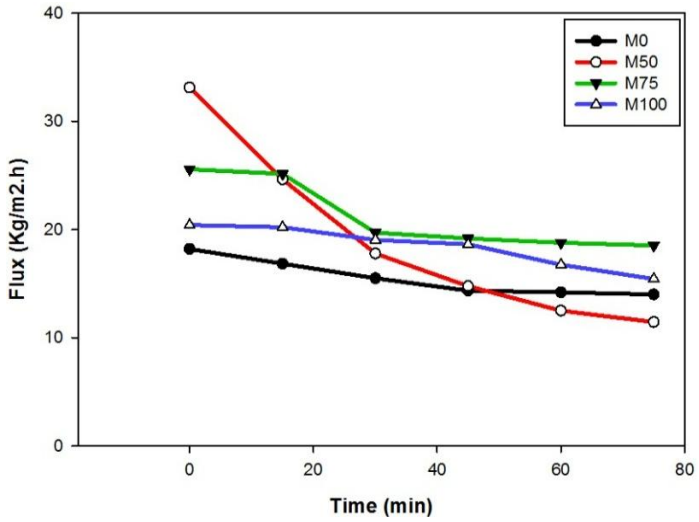

Fig. 10 Flux of different membranes during filtration of whey at long times

Fig. 10 showed the whey flux behavior of the PSf/SPES membranes during whey filtration at long times. It can be seen that all membranes exhibited common trend during long time filtration. The flux of whey diminished at first and eventually it became stable. This could be attributed to concentration polarization and membrane fouling. Whereas M_{50} showed another trend the flux declined during filtration process gradually. Among the membranes containing SPES, M_{100} has lower flux decline during the long time filtration. Therefore, the pore blocking took place a long time during whey filtration.

Comparisons of the proteins rejection of fabricated membranes are illustrated in Fig. 11. This figure expresses that highest and lowest value of proteins rejection related to M_{100} and M_{50} respectively. This can be attributed to the size of the pores of these membranes that M_{100} have lowest pore size and M_{50} have highest pore size. Therefore, most of proteins molecule cannot pass from the pores of M_{100}.

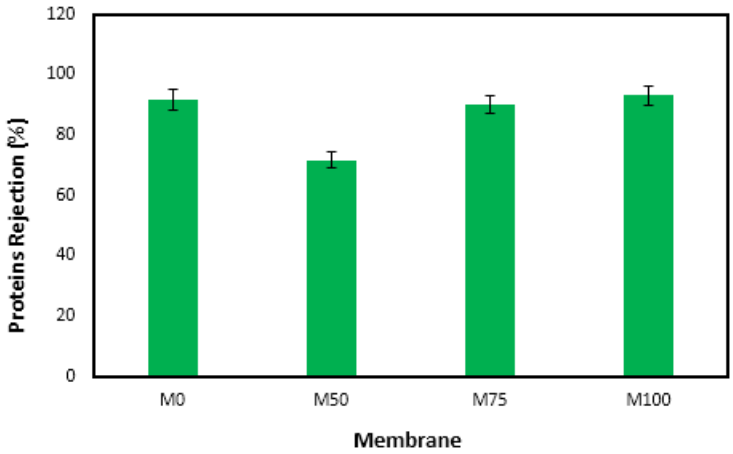

Fig. 11 The effect of SPES on whey proteins removal

Table 4 Flux recovery ratio and resistances of pure and blend membranes

Mem	J_{w0} (kg/m^2.h)	J_p (kg/m^2.h)	J_{w1} (kg/m^2.h)	*FRR* (%)	R_t	R_r	R_{ir}
M_0	74.76	17.56	52.49	70.39	0.76	0.47	0.3
M_{50}	191.79	33.14	56.66	29.55	0.82	0.11	0.7
M_{75}	97.77	24.29	45.05	46.08	0.75	0.21	0.54
M_{100}	43.78	17.19	40.11	91.63	0.61	0.52	0.08

3.6 Analysis the fouling of PSf/SPES membranes

The membrane fouling greatly depends on the blockage or plugging of pores within the membrane as well as the concentration polarization and cake layer formation on the membrane surface (Fane and Fell 1987). Membrane fouling is greatly governed by many causes such as hydrophobic interaction and electrostatic interaction between organic components in the feed and membrane surface, surface porosity and roughness, pore size distribution (Koo *et al*. 2012).

To investigate the fouling properties of membranes, the flux recovery ratio, reversible and irreversible resistance of membranes were calculated and listed in Table 4. The higher flux recovery ratio and lower resistance signified the more antifouling property of membrane. It can be seen that the maximum amount of FRR and lower resistance is attributed to M_{100}. The FRR of this membrane was strongly increased to 91.63%. The higher FRR demonstrated that this membrane have high recycling property. Moreover, lower value of R_t showed that less proteins of whey stick on the membrane surface and pore walls.

In order to better challenge about the concept of antifouling properties of the modified membranes, reversible and irreversible resistance of membranes of SPES/PSf blend membranes was compared with the number of studies which have been published before about the modification of membrane. According to this Table, The irreversible fouling (R_{ir}) of blended membranes (M_{50} and M_{75}) was more than the R_{ir} of single polymer membranes. It seems that M_{50} and M_{75} due to the segregation on their surface have more tendencies to adsorption of whey proteins in the boundary of membrane domains. Irreversible fouling, in which the foulants are firmly bound to the membrane can only be removed by chemical cleaning. Therefore, this type of fouling causes an increase in operational complexity and reduction of membrane lifetime (Peldszus *et al*. 2011, Zinadini *et al*. 2014).

4. Conclusions

Sulfonated polyethersulfone was synthesized by sulfuric acid and used in the casting solution to modify the surface hydrophilicity of ultrafiltration membrane by blending with PSf. The effect of SPES addition in the casting solution on the membranes' structure, morphology, and performance was investigated. The surface SEM images of membranes showed that formed segregation between two polymers on the surface of PSf/SPES blended membrane and neat PSf and SPES membrane have uniform surface. The cross sectional images also indicated that the thickness of dense skin layer increased by addition SPES. The presence of functional hydrophilic groups in the SPES improved the surface hydrophilicity of membrane. The contact angle of modified membranes with SPES was lower than the membrane just including PSf except M_4 that is related to surface roughness. The pure water and whey permeability increased for PSf/SPES membrane

with composition ratio 50/50 (M_{50}) and 25/75 (M_{75}) and decreased for membrane with composition ratio 0/100 (M_{100}) than the membrane just including PSf. Moreover, the proteins rejection of blended membranes is lower than pure PSf and SPES membrane. The hydrophilic surface resulted in enhancement the antifouling properties for neat SPES membrane compared to neat PSf membrane. Among all membranes, the lowest fouling and total resistance was for M100 but M75 has higher flux of whey filtration.

References

Alpatova, A., Kim, E.-S., Sun, X., Hwang, G., Liu, Y. and El-Din, M.G. (2013), "Fabrication of porous polymeric nanocomposite membranes with enhanced anti-fouling properties: Effect of casting composition", *J. Membr. Sci.*, **444**, 449-460.

Argüello, M., Alvarez, S., Riera, F. and Alvarez, R. (2003), "Enzymatic cleaning of inorganic ultrafiltration membranes used for whey protein fractionation", *J. Membr. Sci.*, **216**(1-2), 121-134.

Arthanareeswaran, G., Latha, C., Mohan, D., Raajenthiren, M. and Srinivasan, K. (2006), "Studies on cellulose acetate/low cyclic dimmer polysulfone blend ultrafiltration membranes and their applications", *J. Separ. Sci. Technol.*, **41**(13), 2895-2912.

Baldasso, C., Barros, T. and Tessaro, I. (2011), "Concentration and purification of whey proteins by ultrafiltration", *Desalination*, **278**(1-3), 381-386.

Blanco, J., Nguyen, Q. and Schaetzel, P. (2001), "Novel hydrophilic membrane materials: sulfonated polyethersulfone Cardo", *J. Membr. Sci.*, **186**(2), 267-279.

Bottino, A., Capannelli, G., Munari, S. and Turturro, A. (1988), "High performance ultrafiltration membranes cast from LiCl doped solutions", *Desalination*, **68**(2-3), 167-177.

Chakrabarty, B., Ghoshal, A. and Purkait, M. (2008), "Effect of molecular weight of PEG on membrane morphology and transport properties", *J. Membr. Sci.*, **309**(1-2), 209-221.

Corbatón-Báguena, M.-J., Á lvarez-Blanco, S. and Vincent-Vela, M.-C. (2015), "Fouling mechanisms of ultrafiltration membranes fouled with whey model solutions", *Desalination*, **360**, 87-96.

Costa, A.R., de Pinho, M.N. and Elimelech, M. (2006), "Mechanisms of colloidal natural organic matter fouling in ultrafiltration", *J. Membr. Sci.*, **281**(1-2), 716-725.

Das, B., Sarkar, S., Sarkar, A., Bhattacharjee, S. and Bhattacharjee, C. (2015), "Recovery of whey proteins and lactose from dairy waste: A step towards green waste management", *Process Safety and Environmental Protection*. [In Press]

De Souza, R.R., Bergamasco, R., da Costa, S.C., Feng, X., Faria, S.H.B. and Gimenes, M.L. (2010), "Recovery and purification of lactose from whey", *Chem. Eng. Process.: Process Intensif.*, **49**(11), 1137-1143.

Faibish, R.S. and Cohen, Y. (2001), "Fouling and rejection behavior of ceramic and polymer-modified ceramic membranes for ultrafiltration of oil-in-water emulsions and microemulsions", *Colloid. Surf. A: Physicochem. Eng. Asp.*, **191**(1-2), 27-40.

Fane, A. and Fell, C. (1987), "A review of fouling and fouling control in ultrafiltration", *J. Desal.*, **62**, 117-136.

Hinkova, A., Zidova, P., Pour, V., Bubnik, Z., Henke, S., Salova, A. and Kadlec, P. (2012), "Potential of membrane separation processes in cheese whey fractionation and separation", *Procedia Eng.*, **42**, 1425-1436.

Indok Nurul Hasyimah, M., Mohammad, A. and Markom, M. (2011), "Influence of triglycerides on fouling of glycerol–water with ultrafiltration membranes", *Ind. Eng. Chem. Res.*, **50**(12), 7520-7526.

Jacob, K.N., Kumar, S.S., Thanigaivelan, A., Tarun, M. and Mohan, D. (2014), "Sulfonated polyethersulfone-based membranes for metal ion removal via a hybrid process", *J. Mater. Sci.*, **49**(1), 114-122.

James, B.J., Jing, Y. and Chen, X.D. (2003), "Membrane fouling during filtration of milk—a microstructural

study", *J. Food Eng*.., **60**(4), 431-437.
Jung, Y.C. and Bhushan, B. (2006), "Contact angle, adhesion and friction properties of micro-and nanopatterned polymers for super hydrophobicity", *Nanotechnology*, **17**(19), 4970.
Kesting, R.E. (1965), "Semipermeable membranes of cellulose acetate for desalination in the process of reverse osmosis. I. Lyotropic swelling of secondary cellulose acetate", *J. Appl. Polym. Sci.*, **9**(2), 663-688.
Kiadehi, A.D., Rahimpour, A., Jahanshahi, M. and Ghoreyshi, A.A. (2015), "Novel carbon nano-fibers (CNF)/polysulfone (PSf) mixed matrix membranes for gas separation", *J. Ind. Eng. Chem.*, **22**, 199-207.
Kim, E.-S., Yu, Q. and Deng, B. (2011), "Plasma surface modification of nanofiltration (NF) thin-film composite (TFC) membranes to improve anti organic fouling", *J. Appl. Surf. Sci.*, **257**(23), 9863-9871.
Klaysom, C., Ladewig, B.P., Lu, G.M. and Wang, L. (2011), "Preparation and characterization of sulfonated polyethersulfone for cation-exchange membranes", *J. Membr. Sci.*, **368**(1-2), 48-53.
Koo, C.H., Mohammad, A.W. and Talib, M.Z.M. (2012), "Review of the effect of selected physicochemical factors on membrane fouling propensity based on fouling indices", *Desalination*, **287**, 167-177.
Lalia, B.S., Kochkodan, V., Hashaikeh, R. and Hilal, N. (2013), "A review on membrane fabrication: Structure, properties and performance relationship", *Desalination*, **326**, 77-95.
Lee, H.J., Won, J., Lee, H. and Kang, Y.S. (2002), "Solution properties of poly (amic acid)–NMP containing LiCl and their effects on membrane morphologies", *J. Membr. Sci.*, **196**(2), 267-277.
Li, H., Shi, W., Zhang, Y. and Zhou, R. (2015), "Comparison study of the effect of blending method on PVDF/PPTA blend membrane structure and performance", *Membr. Water Treat., Int. J.*, **6**(3), 205-224.
Ma, H., Bowman, C.N. and Davis, R.H. (2000), "Membrane fouling reduction by backpulsing and surface modification", *J. Membr. Sci.*, **173**(2), 191-200.
Majeed, S., Fierro, D., Buhr, K., Wind, J., Du, B., Boschetti-de-Fierro, A. and Abetz, V. (2012), "Multi-walled carbon nanotubes (MWCNTs) mixed polyacrylonitrile (PAN) ultrafiltration membranes", *J. Membr. Sci.*, **403**, 101-109.
Mohammadi, T., Madaeni, S. and Moghadam, M. (2003), "Investigation of membrane fouling", *Desalination*, **153**(1-3), 155-160.
Pan, K., Song, Q., Wang, L. and Cao, B. (2011), "A study of demineralization of whey by nanofiltration membrane", *Desalination*, **267**(2-3), 217-221.
Patri, M., Hande, V.R., Phadnis, S., Somaiah, B., Roychoudhury, S. and Deb, P. (2004), "Synthesis and characterization of SPE membrane based on sulfonated FEP-g-acrylic acid by radiation induced graft copolymerization for PEM fuel cell", *Polym. Adv. Technol.*, **15**(5), 270-274.
Peldszus, S., Hallé, C., Peiris, R.H., Hamouda, M., Jin, X., Legge, R.L., Budman, H., Moresoli, C. and Huck, P.M. (2011), "Reversible and irreversible low-pressure membrane foulants in drinking water treatment: identification by principal component analysis of fluorescence EEM and mitigation by biofiltration pretreatment", *Water Res.*, **45**(16), 5161-5170.
Peyravi, M., Rahimpour, A. and Jahanshahi, M. (2015), "Developing nanocomposite PI membranes: Morphology and performance to glycerol removal at the downstream processing of biodiesel production", *J. Membr. Sci.*, **473**, 72-84.
Pieracci, J., Crivello, J.V. and Belfort, G. (1999), "Photochemical modification of 10 kDa polyethersulfone ultrafiltration membranes for reduction of biofouling", *J. Membr. Sci.*, **156**(2), 223-240.
Qin, P., Hong, X., Karim, M.N., Shintani, T., Li, J. and Chen, C. (2013), "Preparation of poly (phthalazinone-ether-sulfone) sponge-like ultrafiltration membrane", *Langmuir*, **29**, 4167-4175.
Qiu, S., Wu, L., Pan, X., Zhang, L., Chen, H. and Gao, C. (2009), "Preparation and properties of functionalized carbon nanotube/PSF blend ultrafiltration membranes", *J. Membr. Sci.*, **342**(1-2), 165-172.
Rahimpour, A., Madaeni, S.S., Jahanshahi, M., Mansourpanah, Y. and Mortazavian, N. (2009a), "Development of high performance nano-porous polyethersulfone ultrafiltration membranes with hydrophilic surface and superior antifouling properties", *J. Appl. Surf. Sci.*, **255**(22), 9166-9173.
Rahimpour, A., Madaeni, S., Zereshki, S. and Mansourpanah, Y. (2009b), "Preparation and characterization of modified nano-porous PVDF membrane with high antifouling property using UV photo-grafting", *J. Appl. Surf. Sci.*, **255**(16), 7455-7461.
Rahimpour, A., Jahanshahi, M., Mortazavian, N., Madaeni, S.S. and Mansourpanah, Y. (2010a),

"Preparation and characterization of asymmetric polyethersulfone and thin-film composite polyamide nanofiltration membranes for water softening", *J. Appl. Surf. Sci.*, **256**(6), 1657-1663.

Rahimpour, A., Madaeni, S.S., Ghorbani, S., Shockravi, A. and Mansourpanah, Y. (2010b), "The influence of sulfonated polyethersulfone (SPES) on surface nano-morphology and performance of polyethersulfone (PES) membrane", *J. Appl. Surf. Sci.*, **256**(1), 1825-1831.

Rice, G., Barber, A., O'Connor, A., Stevens, G. and Kentish, S. (2009), "Fouling of NF membranes by dairy ultrafiltration permeates", *J. Membr. Sci.*, **330**(1-2), 117-126.

Shibata, M., Kobayashi, T. and Fujii, N. (2000), "Porous nylon-6 membranes with dimethylamino groups for low pressure desalination", *J. Appl. Polim. Sci.*, **75**(12), 1546-1553.

Sinha, M. and Purkait, M. (2015), "Preparation of fouling resistant PSF flat sheet UF membrane using amphiphilic polyurethane macromolecules", *Desalination*, **355**, 155-168.

Suárez, E., Lobo, A., Álvarez, S., Riera, F.A. and Álvarez, R. (2006), "Partial demineralization of whey and milk ultrafiltration permeate by nanofiltration at pilot-plant scale", *Desalination*, **198**(1-3), 274-281.

Tsakali, E., Petrotos, K., D'Allessandro, A. and Goulas, P. (2010), "A review on whey composition and the methods used for its utilization for food and pharmaceutical products", *Proceedings of the 6th International Conference on Simulation and Modelling in the Food and Bio-Industry* (*FOODSIM 2010*), CIMO, Braganca, Portugal, June.

Wang, D., Li, K. and Teo, W. (2000), "Porous PVDF asymmetric hollow fiber membranes prepared with the use of small molecular additives", *J. Membr. Sci.*, **178**(1-2), 13-23.

Wang, T., Zhao, C., Li, P., Li, Y. and Wang, J. (2015), "Effect of non-solvent additives on the morphology and separation performance of poly (m-phenylene isophthalamide) (PMIA) hollow fiber nanofiltration membrane", *Desalination*, **365**, 293-307.

Wu, G., Gan, S., Cui, L. and Xu, Y. (2008), "Preparation and characterization of PES/TiO_2 composite membranes", *J. Appl. Surf. Sci.*, **254**(21), 7080-7086.

Xing, P., Robertson, G.P., Guiver, M.D., Mikhailenko, S.D., Wang, K. and Kaliaguine, S. (2004), "Synthesis and characterization of sulfonated poly (ether ether ketone) for proton exchange membranes", *J. Membr. Sci.*, **229**(1-2), 95-106.

Yang, S. and Silva, E. (1995), "Novel products and new technologies for use of a familiar carbohydrate, milk lactose", *J. Dairy Sci.*, **78**(11), 2541-2562.

Yorgun, M., Balcioglu, I.A. and Saygin, O. (2008), "Performance comparison of ultrafiltration, nanofiltration and reverse osmosis on whey treatment", *Desalination*, **229**(1-3), 204-216.

Zhao, C., Xu, X., Chen, J. and Yang, F. (2013), "Effect of graphene oxide concentration on the morphologies and antifouling properties of PVDF ultrafiltration membranes", *J. Environ. Chem. Eng.*, **1**(3), 349-354.

Zinadini, S., Zinatizadeh, A.A., Rahimi, M., Vatanpour, V. and Zangeneh, H. (2014), "Preparation of a novel antifouling mixed matrix PES membrane by embedding graphene oxide nanoplates", *J. Membr. Sci.*, **453**, 292-301.

CC